

LETTERS

Evidence for warmer interglacials in East Antarctic ice cores

L. C. Sime¹, E. W. Wolff¹, K. I. C. Oliver^{2†} & J. C. Tindall³

Stable isotope ratios of oxygen and hydrogen in the Antarctic ice core record have revolutionized our understanding of Pleistocene climate variations and have allowed reconstructions of Antarctic temperature over the past 800,000 years (800 kyr; refs 1, 2). The relationship between the D/H ratio of mean annual precipitation and mean annual surface air temperature is said to be uniform $\pm 10\%$ over East Antarctica³ and constant with time $\pm 20\%$ (refs 3–5). In the absence of strong independent temperature proxy evidence allowing us to calibrate individual ice cores, prior general circulation model (GCM) studies have supported the assumption of constant uniform conversion for climates cooler than that of the present day^{3,5}. Here we analyse the three available 340 kyr East Antarctic ice core records alongside input from GCM modelling. We show that for warmer interglacial periods the relationship between temperature and the isotopic signature varies among ice core sites, and that therefore the conversions must be nonlinear for at least some sites. Model results indicate that the isotopic composition of East Antarctic ice is less sensitive to temperature changes during warmer climates. We conclude that previous temperature estimates from interglacial climates are likely to be too low. The available evidence is consistent with a peak Antarctic interglacial temperature that was at least 6 K higher than that of the present day—approximately double the widely quoted 3 ± 1.5 K (refs 5, 6).

Studies have shown that, in simple cases, the stable isotope composition of oxygen and hydrogen (δ ; see Methods) in precipitation is controlled by the temperature difference between the evaporation site and the condensation site, owing to temperature dependent fractionation processes⁷. The δ value of ice in high latitude ice cores is therefore used as a proxy for past temperatures^{7,8}. Past core site surface temperature (T) is obtained from δ by applying an estimated ‘palaeothermometer’ gradient a :

$$\frac{\partial(\delta)}{\partial T} = a \quad (1)$$

Temporally constant and almost geographically invariant East Antarctic gradients have previously been applied in conversions of δ into T . Dome C, Vostok and Dome F ice core δ was converted to temperature using a palaeothermometer gradient of 6‰ per K (ref. 5) or 6.4‰ per K (ref. 4), for δD . These conversions imply that past interglacial T peaked at about 3 ± 1.5 K above the present day temperature at these core sites^{5,6}.

The past 340 kyr of the δ record from the three deep East Antarctic ice cores^{5,9} are shown on the EDC3 (EPICA Dome C) timescale¹⁰ in Fig. 1. Similarities to the deep-sea isotope record¹¹ suggest that these δ timeseries record aspects of global climate. However, individual ice core δ values diverge significantly in time. Dome F attains maximum

peak interglacial values 20–140% higher than Dome C referenced to the present. For the 340 kyr records, the most widely geographically separated pair of Dome C and Dome F ice core δ values show the largest differences.

To explore the reasons for these differences, we calculate the temporal gradients in δ at each site. We then compare the gradient at each location (x, y) to that at Dome C:

$$R_{\delta}(x, y, t) = \frac{\dot{\delta}(x, y, t)}{\dot{\delta}(x_0, y_0, t)} = R_T(x, y, t)R_a(x, y, t) \quad (2)$$

$$R_T(x, y, t) = \frac{\dot{T}(x, y, t)}{\dot{T}(x_0, y_0, t)}, \quad R_a(x, y, t) = \frac{a(x, y, t)}{a(x_0, y_0, t)}$$

where (x_0, y_0) is the location of Dome C and overdots (for example, $\dot{\delta}$) denote differentiation with respect to time. This shows that R_{δ} is the product of two components: the first (R_T) due to geographical variability in the rate of change of temperature, and the second (R_a) due to geographical variability in the palaeothermometer gradient a . When R_{δ} is one, there is no geographical variation in δ in the East Antarctic; R_{δ} above (below) one indicates that the ice core site δ is higher (lower) than the Dome C record.

Cold climate R_{δ} median values of around 0.8 (Fig. 2, left side) indicate that a δ change of 1‰ at Dome C tends to coincide with a

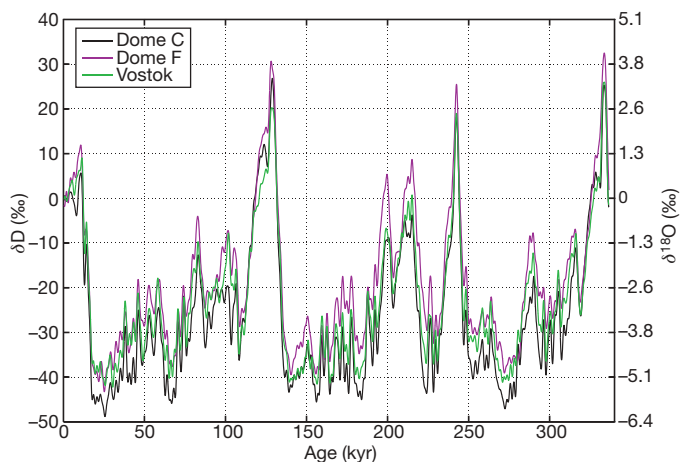


Figure 1 | Time series of Dome C, Dome F and Vostok ice core δ records from preindustrial times until 336.5 kyr ago. All time series are on the EDC3 timescale¹⁰, on a 0.1 kyr interval. The records are presented as anomalies from the present day. See Methods for details of δ .

¹British Antarctic Survey, Cambridge CB3 0ET, UK. ²Department of Earth and Environmental Sciences, The Open University, Milton Keynes MK 7 6AA, UK. ³School of Geographical Sciences, University of Bristol, University Road, Bristol BS8 1SS, UK. †Present address: School of Ocean and Earth Science, National Oceanography Centre, University of Southampton, Southampton SO14 3ZH, UK.

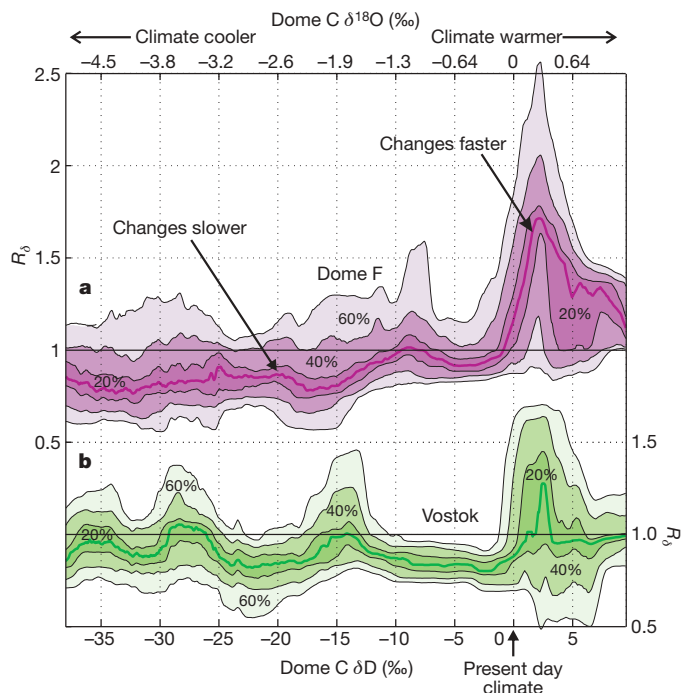


Figure 2 | Observed ice core R_δ against δ . Here R_δ is the ratio of δ at Dome F (a) or at Vostok (b) relative to that at Dome C; the upper and lower x axes show respectively Dome C $\delta^{18}\text{O}$ and Dome C δD . The shading around each R_δ value shows the 20%, 40% and 60% envelope of the R_δ observations. We do not show R_δ for $\delta\text{D} < -38\text{‰}$ or $> 8\text{‰}$ because of insufficient observations of R_δ . R_δ is binned according to Dome C δ with an approximately uniform δ bin width for each sample (see Methods).

change of 0.8‰ at Dome F and Vostok. However, during warmer interglacial periods (Fig. 2, right side), Dome F δ exhibits much stronger variation than Dome C, indicated by R_δ values above 1.

Vostok R_δ has a qualitatively similar but much weaker warm climate R_δ peak. During past warm periods, with δD isotopic values 0–7‰ above present day values, a change of 1‰ at Dome C tends to coincide with a change of 1.4–1.7‰ at Dome F. However, from the observed R_δ ratio we cannot a priori deduce to what extent spatial variability in temperature change, R_T , or in the palaeothermometer gradient, R_a , determine R_δ .

Isotope enabled GCM palaeoclimate experiments provide a powerful means for unravelling the causes of geographical variations in δ across East Antarctica. The isotopic GCM¹² we use has a good representation of the present day global¹³ and Antarctic climate¹⁴, and isotope distribution^{12,15} (see Supplementary Information). Modelled values for East Antarctic R_δ , R_T and R_a are obtained using experiments representing the present day¹⁶, Last Glacial Maximum (LGM)¹⁷, and climates between 0.5 K and 3 K warmer than the modelled present day Dome C temperatures. Because current GCM experiments, using insolation and greenhouse-gas levels appropriate for the last interglacial (125–130 kyr ago), fail to reproduce warmer Southern Hemisphere¹⁸ and Antarctic temperatures¹⁹, we drive our warmer climate experiments instead with higher greenhouse-gas levels.

GCM experiment results in Fig. 3 indicate that geographical variability in temperature change R_T is small compared to geographical variability in the palaeothermometer R_a for both cooler and warmer climates. Additional GCM results²⁰ and independent calculations of R_T using GCM output confirm that R_T is small (see Supplementary Information) compared to observed R_δ . The spatially invariant rates of temperature change shown also suggest that relative accumulation changes between the sites are likely to be small, implying that relative elevation changes between the sites are also small. Analysis of our experiments support this: Dome F precipitation for the present day and all warmer experiments remains constantly $17 \pm 4 \text{ m kyr}^{-1}$ water equivalent lower than Dome C. Therefore we would expect relative elevation changes between the sites for the modelled warmed climates should be within $\pm 4 \text{ m kyr}^{-1}$. From these results we conclude that

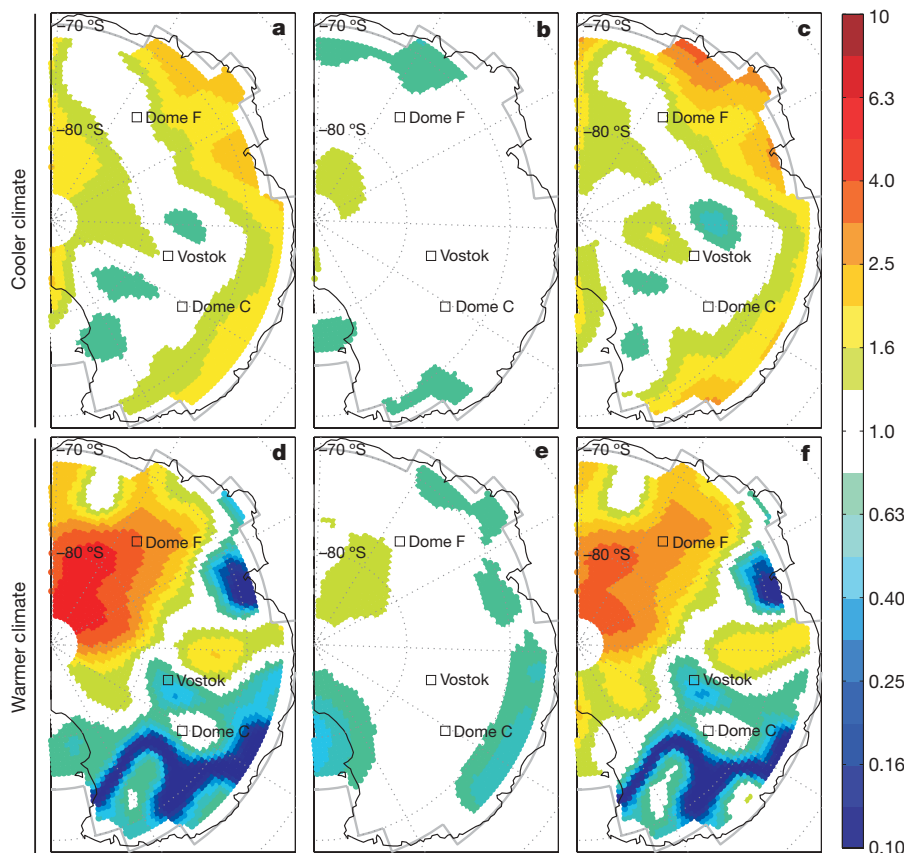


Figure 3 | The geographical pattern of δ , separated into a temperature change component R_T and a palaeothermometer component R_a . a, Mean R_δ (colour coded) between the present day and LGM climate (this is a discrete value calculated from the change between the modelled climates). b, c, As a but showing R_T and R_a respectively. We note that $\log R_\delta = \log R_T + \log R_a$. d–f, As a–c but for a change between the present day and a 3 K warmer (at Dome C) climate. All geographical ratios are referenced to the Dome C core site, hence Dome C R values are all 1. Results are shown using a logarithmic colour scale, and are calculated using values of δ and T with a 300 km radius averaging¹⁵.

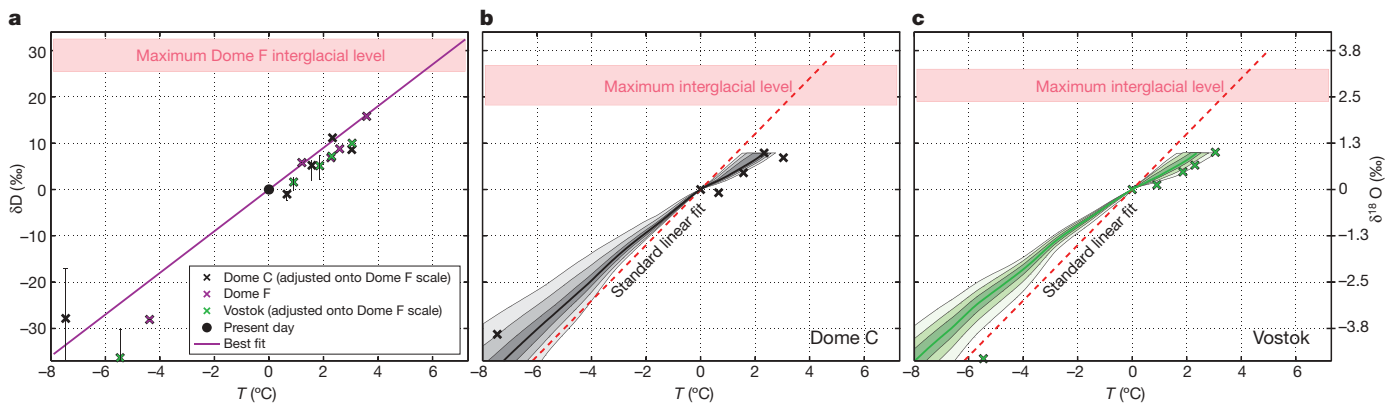


Figure 4 | The δ versus T palaeothermometer relationship. **a**, Dome F model results (magenta), and model results for the other sites normalized to Dome F by the median measured R_δ for the appropriate temperature. The line is the best fit through all the data, constrained to the zero point (see Methods). Error bars show the outer envelope (envelopes are shown in Fig. 2) for each normalization. **b**, **c**, Actual model results (crosses) for Dome C

high plateau East Antarctic R_T is small and thus, for East Antarctic ice cores, R_a is the dominant component of R_δ .

The finding that R_δ approximately equals R_a suggests that the observed differences in the ice core δ records (Fig. 1) can be explained primarily by variations in the palaeothermometer gradient, rather than in temperature. Therefore, the standard approach of applying a constant palaeothermometer gradient must introduce errors to temperature reconstructions for at least two of the three core sites. Although probably too simple, the least complex assumption that is consistent with the data are that one site has a constant gradient, and can be treated as a reference site. We then normalize model δ values for the other sites to those of the reference, using integrated observed R_δ values for the appropriate temperature shown Fig. 2; this allows us to use the model results from all three sites together to make a best estimate of temperature changes (see Methods Summary). Using this approach, we find that the best least squares fit is obtained if the Dome F site has a constant gradient; this gives a palaeothermometer gradient of $4.5 \pm 1.1\%$ per K (Fig. 4). This gradient and the uncertainties calculated (see Methods) imply that maximum interglacial temperatures over the past 340 kyr were between 6.0 K and 10.0 K above present-day values (Fig. 4a).

Detailed analysis of GCM experiments shows trends in covariance between surface temperature and precipitation throughout the modelled warming¹⁵, which can affect ice core δ records⁷. The seasonal and synoptic covariance changes have a limited impact on the geographical warming pattern R_T (refs 15, 21), but are sufficient to explain our climate dependence of the δ against T relationship. Warmer climates are associated with a larger proportion of precipitation in cold seasons over Dome C and Vostok¹⁵. This effectively reduces the condensation temperature change relative to the mean annual temperature change, lowering the palaeothermometer gradient at these sites for warm climates compared to cold climates. Over the Dome F sector, trends in high pressure blocking events have been observed over the past two decades^{21,22}. Similarly, modelled synoptic trends in covariance occur in the GCM experiments over the Dome F sector¹⁵ and act to raise the warm climate palaeothermometer gradient in this region. These changes in covariance make the Dome F δ response to T more weakly nonlinear, thus the constant Dome F conversion of δ to T is a better approximation than a constant conversion for Dome C or Vostok.

The majority of the present day precipitation falling across the East Antarctic Plateau, which accumulates to form ice cores, is evaporated from the Atlantic and Indian sectors of the Southern Ocean^{23,24}. Changes in the evaporative source characteristics are thought to be relatively small for our core sites during climate shifts^{25,26}.

(b) and Vostok (c), and the best fit in a adjusted according to the observed R_δ . The median R_δ and envelope used are shown in Fig. 2. In b and c, the red dashed line shows the standard^{4,5} conversion line $a = 6\delta D$, where a is in units of $\%$ per K. The range of maximum interglacial core site δ values are indicated on each panel.

Additionally, because the source vapour is from a common region, changes in source temperature or humidity affect East Antarctic Plateau precipitation uniformly during climate changes. For this reason evaporative source changes do not qualitatively affect the analysis above: applying a constant palaeothermometer gradient introduces errors in two of the three sites, regardless of any source temperature or humidity changes. Most uncertainty in the relationship between warm period temperature and δ is due to changes in the Antarctic accumulation regime¹⁵, described in the previous paragraph, and complex atmospheric mixing changes such as those induced by warm climate differences in sea-ice and rates of atmospheric overturning^{27,28}. Analysis of additional warm period GCM experiments, which feature different warm climate sea-ice, sea surface temperatures, and precipitation regimes, indicate that these warm period climate differences contribute $\pm 1.1\%$ per K to the gradient (see Online Methods).

An interglacial temperature of the level suggested by Fig. 4 indicates that there are serious deficiencies in our understanding of warmer than present day climates^{18,19}. It may be that ice sheet elevation changes outside the East Antarctic, such as the possible loss of the West Antarctic ice-sheet²⁹, or changes in sea surface temperatures and sea-ice, have contributed to the past high interglacial East Antarctic temperatures. Coupled ocean-atmosphere GCM experiments could throw light on the causes of these high East Antarctic temperatures. The analysis presented here can be used to assess the results of such modelling studies. However, further proxy data on all aspects of interglacial climates would be invaluable. Past interglacials offer the chance to test whether modelled consequences of future polar warming are realistic. It is therefore essential to confirm what temperature level was reached, before one can assess the consequences of such a climate.

METHODS SUMMARY

East Antarctic stable water isotope (deuterium, D, and oxygen-18, ^{18}O) records from 336.5 kyr ago are available for three ice cores^{5,6,9}. Fractional isotopic content is expressed for deuterium as: $\delta D = 1,000 \times [(\text{HD}^{16}\text{O}/\text{H}_2^{16}\text{O})/R_{\text{VSMOW}} - 1]$ (in $\%$), where R_{VSMOW} is the ratio of HD^{16}O to H_2^{16}O for Vienna standard mean ocean water⁸. We use δ as shorthand to represent both δD and $\delta^{18}\text{O}$ (see Online Methods), put all values on the EDC3 timescale¹⁰, and present δ values as anomalies from the present day. Because of differences in the temporal resolution of the records, a 1.5 kyr low-pass filter is used on the δ records to ensure they are equivalent. We use 3 kyr segments to calculate a discrete approximation to δ , and exclude δ values which show sensitivity to ice core synchronization errors. The $\delta(t)$ values are used to calculate $R_\delta(t)$ (equation (2)). Values are then binned according to Dome C $\delta(t)$ to get $R_\delta(\delta)$ (Fig. 2). We use larger sample sizes for colder climates to provide an approximately uniform δ bin width.

A best fit through the GCM experiments (see Supplementary Information), constrained to the zero point, is obtained by calculating the value of a_0 that minimizes $\sum E_{ij}^2$ in

$$\delta_{ij} \int_0^{T_{ij}} (R_{\delta})_{\text{ref}} dT = (a_0 T_{ij} + E_{ij}) \int_0^{T_{ij}} (R_{\delta})_j dT$$

where T_{ij} and δ_{ij} are GCM temperature and δ in simulation i at core site j , jref is the choice of reference site where a constant palaeothermometer gradient is assumed, and R_{δ} at Dome C is 1. The optimal r.m.s. (root-mean-squared) errors using Dome C, Dome F and Vostok as reference sites are 6.0‰, 4.3‰ and 5.1‰, respectively. These r.m.s. values indicate that it is more appropriate to assume a linear relation for Dome F than for the other sites. The method for estimating the uncertainty in a_0 is described in the Online Methods section.

Full Methods and any associated references are available in the online version of the paper at www.nature.com/nature.

Received 9 October 2008; accepted 5 October 2009.

- Solomon, S. *et al.* (eds) *Climate Change 2007: The Physical Science Basis* (Cambridge Univ. Press, 2007).
- EPICA Community Members. Eight glacial cycles from an Antarctic ice core. *Nature* **429**, 623–628 (2004).
- Jouzel, J. *et al.* Magnitude of isotope/temperature scaling for interpretation of central Antarctic ice cores. *J. Geophys. Res.* **108** (D12), 26471–26487 (2003).
- Watanabe, O. *et al.* Homogeneous climate variability across East Antarctica over the past three glacial cycles. *Nature* **422**, 509–512 (2003).
- Jouzel, J. *et al.* Orbital and millennial Antarctic climate variability over the past 800,000 years. *Science* **317**, 793–796 (2007).
- Petit, J. R. *et al.* Climate and atmospheric history of the past 420,000 years from the Vostok ice core, Antarctica. *Nature* **399**, 429–436 (1999).
- Dansgaard, W. Stable isotopes in precipitation. *Tellus* **16**, 436–468 (1964).
- Rozanski, K., Araguas-Araguas, L. & Gonfiantini, R. Relation between long-term trends of oxygen-18 isotope composition of precipitation and climate. *Science* **258**, 981–985 (1992).
- Kawamura, K. *et al.* Northern Hemisphere forcing of climatic cycles in Antarctica over the past 360,000 years. *Nature* **448**, 912–916 (2007).
- Parrenin, F. *et al.* The EDC3 chronology for the EPICA Dome C ice core. *Clim. Past* **3**, 485–497 (2007).
- Lisiecki, L. E. & Raymo, M. E. A Pliocene-Pleistocene stack of 57 globally distributed benthic $\delta^{18}\text{O}$ records. *Paleoceanography* **20**, PA1003, doi:10.1029/2004PA001071 (2005).
- Tindall, J., Valdes, P. & Sime, L. Stable water isotopes in HadCM3: the isotopic signature of ENSO and the tropical amount effect. *J. Geophys. Res.* D04111, doi:10.1029/2008JD010825 (2008).
- Pope, V. D., Gallani, M. L., Rowntree, P. R. & Stratton, R. A. The impact of new physical parametrizations in the Hadley Centre climate model: HadAM3. *Clim. Dyn.* **16**, 123–146 (2000).
- Turner, J., Connolley, W. M., Lachlan-Cope, T. A. & Marshall, G. J. The performance of the Hadley Centre Climate Model (HadCM3) in high southern latitudes. *Int. J. Climatol.* **26**, 91–112 (2006).
- Sime, L. C., Tindall, J., Wolff, E., Connolley, W. & Valdes, P. The Antarctic isotopic thermometer during a CO_2 forced warming event. *J. Geophys. Res.* **113**, D24119, doi:10.1029/2008JD010395 (2008).
- Rayner, N. A. *et al.* Global analyses of sea surface temperature, sea ice, and night marine air temperature since the late nineteenth century. *J. Geophys. Res.* **108** (D14), 4407, doi:10.1029/2002JD002670 (2003).
- Paul, A. & Schäfer-Neth, C. Modeling the water masses of the Atlantic Ocean at the Last Glacial Maximum. *Paleoceanography* **18**, 1058, doi:10.1029/2002PA000783 (2003).
- Otto-Bliessner, B. L. *et al.* Simulating Arctic climate warmth and icefield retreat in the last interglaciation. *Science* **311**, 1751–1753 (2006).
- Groll, N., Widmann, M., Jones, J., Kaspar, F. & Lorenz, S. Simulated differences in the relationships between regional temperatures and large-scale circulation during the early Eemian interglacial (125 kyr BP) and the pre-industrial period. *J. Clim.* **18**, 4035–4048 (2005).
- Bracegirdle, T. J., Connolley, W. M. & Turner, J. Antarctic climate change over the twenty first century. *J. Geophys. Res.* **113**, D03103, doi:10.1029/2007JD008933 (2008).
- Schneider, D. P., Steig, E. J. & Comiso, J. C. Recent climate variability in Antarctica from satellite-derived temperature data. *J. Clim.* **17**, 1569–1583 (2004).
- Hirasawa, N., Nakamura, H. & Yamanouchi, T. Abrupt changes in meteorological conditions observed at an inland Antarctic station in association with wintertime blocking. *Geophys. Res. Lett.* **27**, 1911–1914 (2000).
- Delaygue, G., Jouzel, J., Masson, V., Koster, R. D. & Bard, E. Validity of the isotopic thermometer in central Antarctica: limited impact of glacial precipitation seasonality and moisture origin. *Geophys. Res. Lett.* **27**, 2677–2680 (2000).
- Werner, M., Heimann, M. & Hoffmann, G. Isotopic composition and origin of polar precipitation in present and glacial climate simulations. *Tellus B* **53**, 53–71 (2001).
- Vimeux, F., Masson, V., Jouzel, J., Stievenard, M. & Petit, J. R. Glacial–interglacial changes in ocean surface conditions in the Southern Hemisphere. *Nature* **398**, 410–413 (1999).
- Vimeux, F., Cuffey, K. & Jouzel, J. New insights into Southern Hemisphere temperature changes from Vostok ice cores using deuterium excess correction. *Earth Planet. Sci. Lett.* **203**, 829–843 (2002).
- Noone, D. & Simmonds, I. Sea ice control of water isotope transport to Antarctica and implications for ice core interpretation. *J. Geophys. Res.* **109**, D07105, doi:10.1029/2003JD004228 (2004).
- Noone, D. The influence of midlatitude and tropical overturning circulation on the isotopic composition of atmospheric water vapor and Antarctic precipitation. *J. Geophys. Res.* **113**, D04102, doi:10.1029/2007JD008892 (2008).
- Overpeck, J. T. *et al.* Paleoclimatic evidence for future ice-sheet instability and rapid sea-level rise. *Science* **311**, 1747–1750 (2006).

Supplementary Information is linked to the online version of the paper at www.nature.com/nature.

Acknowledgements We thank W. Connolley for assistance with model set-up; T. Bracegirdle for organizing multi-model AR4 output; NERC RAPID ISOMAP for funding the model development; and the modelling groups, and the Program for Climate Model Diagnosis and Intercomparison (PCMDI) and the WCRP's Working Group on Coupled Modelling (WGCM) for their roles in making available the WCRP CMIP3 multi-model data set.

Author Contributions L.C.S. and E.W.W. discussed the original concept for the work. L.C.S. and K.I.C.O. wrote the ice core R_{δ} analysis. J.C.T. wrote the isotopic code for the HadAM3 model. L.C.S. set up and analysed the isotopic HadAM3 experiments and analysed the additional AR4 GCM output. L.C.S. wrote the paper. All authors discussed the results and modified the manuscript.

Author Information Reprints and permissions information is available at www.nature.com/reprints. Correspondence and requests for materials should be addressed to L.C.S. (lsim@bas.ac.uk).

METHODS

East Antarctic Dome C and Vostok deuterium (D) and Dome F oxygen-18 (^{18}O) records from the preindustrial until 336.5 kyr ago are available at the World Data Center for Paleoclimatology^{5,6,9}. The fractional contents of the stable water isotopes D and ^{18}O are expressed as deviations from a standard water isotope sample, so for deuterium: $\delta\text{D} = 1,000 \times [(\text{HD}^{16}\text{O}/\text{H}_2^{16}\text{O})/R_{\text{VSMOW}} - 1]$ (units are ‰), and for ^{18}O : $\delta^{18}\text{O} = 1,000 \times [(\text{H}_2^{18}\text{O}/\text{H}_2^{16}\text{O})/R_{\text{VSMOW}} - 1]$ (units are ‰), with R_{VSMOW} = the ratio of Vienna standard mean ocean water for each isotopic species⁸. Here we use δ as shorthand to represent both δD and $\delta^{18}\text{O}$.

The timeseries of Dome C, Dome F and Vostok ice core δ records are placed on the EDC3 timescale¹⁰. The timeseries are put on an 0.1 kyr interval. Records are smoothed with a 0.2 kyr running mean to prevent any high frequency aliasing. They are then aligned on the y -axis using the mean of the last 3 kyr of each record, that is, the present day δ of each record, thus δ values are presented as anomalies from the present day. A 1.5 kyr low-pass filtering ensures that changes in the temporal resolution of the records (which drops to 0.65 kyr for older parts of the Dome F record) do not affect the sampling throughout and between the records.

The relationship between $\delta^{18}\text{O}(t)$ and $\delta\text{D}(t)$ is generally presented in terms of a conversion coefficient plus a small temporally varying term, the deuterium excess or $d(t)$ parameter. The conversion is defined here as $\delta\text{D}(t) = d(t) + 7.85 \times \delta^{18}\text{O}(t)$, with no uncertainties, using the East Antarctic coefficient of 7.85 (ref. 25) from the Vostok ice core. The Dome F $d(t)$ record³⁰ can therefore be used to convert the Dome F $\delta^{18}\text{O}(t)$ record into a $\delta\text{D}(t)$ record so that $\delta(t)$ can be directly compared for the three cores. We also use unpublished Dome C $\delta^{18}\text{O}(t)$ and Dome F $\delta\text{D}(t)$ to ensure that no extra errors are introduced into the analysis. The standard deviation of Dome C $d(t)$ is 1.7‰, and of this, 21% of $d(t)$ correlates with $\delta(t)$. Because the standard deviation (a measure of the variance) is very small, we use the mean coefficient of 7.85 to provide results on dual δD and $\delta^{18}\text{O}$ axes. Presenting all δD and $\delta^{18}\text{O}$ values relative to the present day ensures that errors due to using dual axes are minimized. Of this small uncertainty introduced to the axes by $d(t)$, 79% is uncorrelated with $\delta(t)$, so systematic errors associated with the dual axes are negligible compared with the δ ranges considered in this manuscript. Note, as described above, that this negligible dual axes error does not affect the calculated R_δ values.

We use 3 kyr segments of $\delta(t)$ to calculate a discrete approximation to $\dot{\delta}(t)$ for each site, that is, the change in δ through time. The $\dot{\delta}(t)$ values are used to calculate $R_\delta(t)$ (equation (2)), and $R_\delta(t)$ is then binned according to Dome C δ (Fig. 2) to obtain $R_\delta(\delta)$. Because of the high frequency of low $\dot{\delta}(t)$ values, and the low frequency of high $\dot{\delta}(t)$ values, sample sizes are larger for colder climates (sample size 20 kyr at $\delta\text{D} = -37\text{‰}$), and linearly decreases for less depleted (warmer) climates (sample size 4 kyr at $\delta\text{D} = 9\text{‰}$). This gives an approximately uniform bin width.

Because the R_δ analysis of the ice core $\delta(t)$ values is based on ratios of $\dot{\delta}(t)$ (temporal change in δ), R_δ is almost completely independent of absolute age-model accuracy (as R_δ is a geographically relative rather than an absolute measure). Similarly, marine source changes due to ice-sheet volume changes²⁶ do not affect the calculation of R_δ , because all records are affected identically. Likewise, marine source temperature and humidity changes^{25,26} will have little effect on R_δ because they vary little across the plateau^{23,24}. The R_δ analysis will however be sensitive to ice core synchronization errors. We calculate the variability in $\dot{\delta}(t)$ which can be explained by a linear trend in each 3 kyr segment, and do not use

3 kyr segments where more than 50% of the variability in $\dot{\delta}(t)$ in either record is not explained by a linear fit. This limits the analysis to portions of the ice core where both records show a simple linear trend, eliminating very low $\dot{\delta}(t)$ values and times of inflecting $\dot{\delta}(t)$ values (uncertain $\dot{\delta}(t)$). Removing these low and uncertain $\dot{\delta}(t)$ periods from the analysis minimizes the impact of uncertainties in the depth-age model on the calculated R_δ . The use of 3-kyr segments means we are using a discrete approximation to $\dot{\delta}(t)$, which would be unsuitable for examining variability on seasonal to millennial timescales.

We calculate the best fit through all GCM experiments (see Supplementary Information for details of model and boundary conditions), constrained to the zero point, by obtaining the value of a that minimizes $\sum E_{ij}^2$ in

$$(\delta_{ij} + \hat{\delta}_{ij})(I_{j\text{ref}} + \hat{I}_{j\text{ref}}) = (aT_{ij} + E_{ij})(I_j + \hat{I}_j), \quad I_j = \int_0^{T_{ij}} (R_\delta)_j dT$$

where T_{ij} and δ_{ij} are GCM temperature anomalies and δ in simulation i at core site j , $j\text{ref}$ is the choice of reference site where a constant palaeothermometer gradient is assumed, and R_δ at Dome C is 1. $\hat{\delta}$ and \hat{I} are the error in δ and I , and are assumed equal to zero in determining the best estimate gradient a_0 of 4.5‰ K^{-1} with Dome F as the reference site. The optimal r.m.s. values of E_{ij} using Dome C, Dome F and Vostok as reference sites are 6.0‰, 4.3‰ and 5.1‰, respectively. These r.m.s. error values indicate that it is more appropriate to assume a linear relation for Dome F than for the other sites.

Uncertainties associated with this method for estimating the palaeothermometer gradient arise principally by two mechanisms: (1) uncertainty in observational R_δ (see envelopes in Fig. 2), which relates both to observed 'climate noise' and measurement (for example, age-model) noise; and (2) uncertainty in the model palaeothermometer, whereby different climates yielding identical temperatures at a given site may yield different values of δ . These uncertainties are represented in the error terms \hat{I} and $\hat{\delta}$, respectively. A 1,000-member Monte Carlo analysis is used to obtain a distribution of palaeothermometer gradients resulting from applying values of \hat{I}_{ij} and $\hat{\delta}_{ij}$ randomly selected from Gaussian distributions. The distribution for \hat{I} is determined using median R_δ values (presented in Fig. 2), and observed δ at Dome F, to estimate δ at Dome C and Vostok. The r.m.s. error in this estimate of δ , compared to observed δ , is 4.4‰ at Dome C and 3.5‰ at Vostok. In order to estimate the 'climate error' distribution $\hat{\delta}$, we obtain values of δ at each core site from four additional experiments targeted at 2100 climate (Supplementary Information). These experiments provide an estimate of a Gaussian distribution of δ consistent with a specific change in temperature. The standard deviations are 4.6‰, 8.1‰ and 3.7‰, for Dome C, Dome F and Vostok, respectively. We assume that all errors are uncorrelated. This leads to a pessimistic error estimate for the palaeothermometer gradient because positively correlated errors tend to alter the mean value of δ rather than its gradient. Nevertheless, 95% of palaeothermometer gradient estimates, resulting from the Monte Carlo analysis, fall between 3.2‰ K^{-1} and 5.4‰ K^{-1} . These gradients lead to the range of maximum interglacial temperatures between 6.0 K and 10.0 K above present-day.

30. Uemura, R., Yoshida, N., Kurita, N., Nakawo, M. & Watanabe, O. An observation-based method for reconstructing ocean surface changes using a 340,000-year deuterium excess record from the Dome Fuji ice core, Antarctica. *Geophys. Res. Lett.* 31, doi:10.1029/2004GL019954 (2004).